

Transport properties of random and nonrandom substitutionally disordered alloys. I. Exact numerical calculation of the ac conductivity

M. Hwang, A. Gonis, and A. J. Freeman

Department of Physics and Astronomy and Materials Research Center, Northwestern University, Evanston, Illinois 60201

(Received 24 November 1986)

Results of exact computer simulations for the zero-temperature ac conductivity of one-dimensional substitutionally disordered alloys are reported. These results are obtained by (i) solving for the eigenvalues and eigenvectors of a Hamiltonian associated with a specific configuration of 500 atoms on a linear chain, (ii) evaluating the ac conductivity of this configuration by using the Kubo-Greenwood formula, and (iii) averaging the resulting conductivities over 20 to 50 different configurations (the number of configurations depends on the type of disorder). In all cases convergence (i.e., a stable result) was obtained and confirmed by another independent approach (the recursive method). For not too weak disorder (defined precisely in the text), these results exhibit a great deal of fine structure that includes high peaks and gaps where the conductivity vanishes. These features are reminiscent of, and are correlated with, the similar kind of behavior of the densities of states of one-dimensional substitutionally disordered alloys. Thus we find that the fine structure in the ac-conductivity spectra of one-dimensional systems provides a rigorous testing ground for judging the validity of analytic theories for calculating the transport properties of substitutionally disordered systems.

I. INTRODUCTION

The transport properties of substitutionally disordered alloys are of great technological and theoretical interest, and a great deal of effort has been expended in their study. Most of this effort consists of attempts to generalize well-founded theories for the study of single-particle Green functions of disordered systems to the study of two-particle propagators. This is the first of two papers along this line, concerned specifically with the zero-temperature ac conductivity of substitutionally disordered alloys. The purpose of these investigations is to present exact computer simulations as well as a coherent method for calculating the transport properties away from the mobility edge of substitutionally disordered systems, the ac conductivity in particular.¹ This method is general enough to be applicable to materials describable by Hamiltonians of various kinds including tight-binding (TB) or muffin-tin (MT) potentials, and is characterized by well-defined, controlled levels of approximation. The method is based on the single-site coherent-potential approximation^{2,3} (CPA) and some of its generalizations,⁴⁻⁸ in particular the embedded-cluster method,^{7,8} which have proved very successful in calculating single-particle properties such as the density of states (DOS) of elementary excitations in substitutionally disordered systems. It is our purpose to bring the calculation of the two-particle properties (transport properties) of such systems on a par with corresponding calculations of the single-particle properties.

Analytic methods for the approximate evaluation of the single-particle Green function associated with substitutionally disordered systems⁹ have been developed in conjunction with the existence of a large number of experi-

mental results and computer simulations. Comparison of the results of experiments with those of theory serve as a guide in sorting out such theories on the basis of accuracy and physical content. When coupled with the requirements of analyticity and computational feasibility such comparisons become a powerful tool in testing and directing the development of alloy theory. As a result, there has evolved a selected number of approximate methods that have withstood these tests, and so allow the rather accurate determination of the DOS's of substitutionally disordered alloys. It is particularly the comparisons of theoretical results with those of exact computer simulations for disordered one-dimensional materials that have provided the most severe tests and have caused the demise of several, originally promising, approximations.

In contrast, although there exists¹⁰ a wealth of experimental information on the ac conductivity of disordered alloys that spans the entire concentration range for many systems, we have been unable to find comparable first-principles calculations of the ac conductivity. Similarly, only scanty information is available on the ac conductivity of model disordered systems through computer simulations. This has prohibited direct and meaningful tests of analytic, approximate theories. It is the purpose of this first paper to provide, as comprehensively as possible, a set of simulation results for the ac conductivity of one-dimensional-model disordered systems that are characterized by various types of disorder and probability distributions. These results will then be used in the following paper¹ as a standard by which to judge the validity and accuracy of various analytic approximations for calculating the transport properties of disordered materials. We also hope that they can be used in a similar manner by other investigators.

The ac conductivity was chosen as the prototype of transport quantities, as well as being computationally reliable in calculations for model disordered systems. Reliable computer simulations of the dc conductivity for a linear chain, on the other hand, require a large sample size¹¹ (10^5 sites) and thus far have made useful computations extremely difficult. (This difficulty is associated with the localization property of electronic states in disordered systems.) The calculation of the ac conductivity, however, bypasses the localization problem via the assistance of photon-stimulated conduction.

The zero-temperature ac conductivity of one-dimensional disordered systems was studied in three previous computer simulations.^{12–14} In the first simulation,¹² a single array of randomly positioned δ -function potentials was considered in an attempt to study the transport properties of structurally disordered systems. This work focused on the low-frequency conductivity and averaged the ac conductivity over ten configurations. The authors concluded that the conductivity spectrum was not well defined because their results varied drastically from configuration to configuration.

There may have been two reasons for this instability: first, the special choice of the Fermi level as the lowest eigenvalue of the spectrum, i.e., the consideration of a strictly one-electron system; second, the small size of the sample used whereas—as demonstrated—a large sample size is required for investigating the low-frequency conductivity.^{11,14} However, as the second simulation¹³ has shown, if one is interested in the high-frequency regime and does not restrict the Fermi energy to the lowest level, stable results for the ac conductivity can be obtained for a disordered linear chain with about 400, or more, atoms. The averaged ac conductivity converges to well-defined values as the number of configurations increases.

The computer simulations just mentioned do not provide a sufficiently wide basis for the calibration of analytic, approximate theories. We modified and applied the algorithm used in the second computer experiment¹³ to various one-dimensional TB substitutionally disordered systems with various types of disorder and degrees of short-range order. Using the formalism of linear-response theory, we calculated the ac conductivity on the basis of the Kubo-Greenwood formula. For not too weak disorder, the results exhibit a great deal of fine structure that includes high peaks and gaps where the conductivity vanishes. These features are reminiscent of the comparable structure of the DOS spectra of one-dimensional substitutionally disordered alloys. Such numerical calculations provide a testing ground for analytic theories, and allow the selection of those approximate methods which can account for the effects of local environment fluctuations and the so-called vertex corrections in the calculation of the transport properties of disordered systems. The vertex corrections can be shown to vanish in the single-site coherent-potential approximation¹⁵ (CPA) for single-band TB systems, but are nonzero in multisite calculations,¹⁶ or for multiband materials.¹⁷ Any satisfactory analytic theory must provide a precise prescription for the calculation of these vertex corrections. In the following paper,¹ the results obtained on the basis of such theories will be

presented and analyzed in comparison with the exact results presented in this paper.

Away from the low-frequency regime we expect that finite-size effects in our simulations are negligible. However, for comparative reasons, we also applied the recursive algorithm used by the third computer experiment,¹⁴ in which these effects are minimized, to calculate the ac conductivity of the same model disordered systems. The results can agree quite well qualitatively and quantitatively with those mentioned above, but the rather strong dependence¹⁴ of the results on the choice of the small imaginary energy part used in this approach may lead to the failure of the fundamental sum rules of the conductivity function. This suggests that the algorithm used by the second computer experiment¹³ is more suitable for the comparative calculations with which we are concerned.

The outline of this paper is as follows. In Sec. II various models concerning one-dimensional substitutionally disordered alloys are defined. A discussion of the role of computer simulations for the ac conductivity and the methodology used in obtaining the results reported in this paper are presented in Sec. III. In Sec. IV we will exhibit these results and discuss various constraints imposed on the simulations. Finally, the results obtained by the recursive method, and the applicability and generalization of our methods are discussed in the last section.

II. MODELS OF SUBSTITUTIONAL DISORDER

Within a single-band TB formalism, the Hamiltonian of a substitutionally disordered alloy can be written in the form

$$H = \sum_i \epsilon_i |i\rangle \langle i| + \sum_{\substack{i,j \\ (i \neq j)}} W_{ij} |i\rangle \langle j|. \quad (2.1)$$

Here, $|i\rangle$ denotes an eigenstate associated with the site i and ϵ_i is a site-diagonal energy which can vary randomly from site to site. The variation of ϵ_i is referred to as diagonal disorder. The transfer integrals W_{ij} represent the hopping strength of an electron from site i to site j and in general depend on the chemical occupations of site i and j , as well as on their local environment. The dependence of W_{ij} on the configuration of an alloy is referred to as off-diagonal disorder (ODD) and reflects the fact that the alloy components are characterized by different bandwidths in their pure states. In random alloys, the species of atoms occupying the sites of a lattice are statistically independent. If the chemical species occupying lattice sites are correlated, the system is said to exhibit short-range order (SRO). In more complicated systems, such as compositionally modulated alloys (CMA's), the concentration of a species varies periodically along a particular direction with a wavelength that is commensurate with the lattice. We consider explicitly several classes of substitutional alloys.

A. Class I: Random disorder

1. Binary alloys

(a) *Diagonal disorder.* Let A and B represent the alloy components of a binary alloy $A_{c_A}B_{c_B}$, where c_A

($c_B = 1 - c_A$) is the concentration of species A (B). The site energy ε_i in Eq. (2.1) can assume the values E_A or E_B , i.e., the site energies characterizing the chemical species A or B . The hopping integrals W_{ij} depend solely on the distance between sites i and j and are independent of the chemical occupation of these sites. The relative magnitude of the difference in site energies and the hopping integral signifies the scattering strength,

$$\delta = \frac{|E_A - E_B|}{w}, \quad (2.2)$$

where w is equal to one-half of the bandwidth of either constituent in a pure system.

(b) *Off-diagonal disorder.* In addition to the random parameters we specified in the case of diagonal disorder, the hopping integral W_{ij} is now also a random variable. In general, the hopping integral depends on the local environment of sites i and j in a very complicated way. We limit ourselves to the case in which W_{ij} depends only on the chemical occupancies of and the distance between sites i and j . If a system possesses only nearest-neighbor interactions, three additional parameters are needed to specify this kind of disorder: the hopping integrals W_{AA} , W_{AB} , and W_{BB} , between two atoms of type A , one A and one B , and two atoms of type B , respectively.

2. Ternary alloys

When the number of alloy components increases, the total number of parameters needed to describe the alloy increases correspondingly. In a ternary (three-component) alloy, the site energy ε_i can be E_A , E_B , or E_C with probabilities c_A , c_B , or c_C , respectively, with $c_A + c_B + c_C = 1$. Diagonally and off-diagonally disordered systems can be defined in the manner indicated in the preceding paragraphs.

B. Class II: Short-range order

Perfect substitutional disorder is seldom achieved: Correlations between atoms on neighboring lattice sites cannot usually be ignored. In a binary alloy, for example, it may be energetically favorable to surround an A atom by B atoms, rather than by atoms of the same type. The resulting system then exhibits what is known as short-range order (SRO) effects. In our calculations, we chose a commonly used description of the degree of SRO in terms of the pair distribution probabilities $P_{\alpha\beta}$, $\alpha, \beta = A, B$, of the occupation of near-neighboring sites. If a site is occupied by an atom of type A , a neighboring site will be occupied by an A atom with a probability P_{AA} and occupied by a B atom with probability P_{AB} . The pair distribution functions of neighboring sites can be defined by the equations

$$\begin{aligned} P_{AA} &= c_A + \alpha(1 - c_A), \\ P_{AB} &= 1 - P_{AA}, \\ P_{BB} &= c_B + \alpha(1 - c_B), \\ P_{BA} &= 1 - P_{BB}, \end{aligned} \quad (2.3)$$

where α is an order parameter with the values $\alpha > 0$ ($\alpha < 0$) signifying clustering (ordering), and $\alpha = 0$ denoting a random alloy. Thus clustering ($\alpha > 0$) refers to the tendency of atoms of a given kind in the alloy to surround themselves by like atoms, whereas ordering ($\alpha < 0$) signifies the opposite effect. Thus for $\alpha = 1$ the alloy separates into pure- A and pure- B phases. For $\alpha = -1$ and $c_A = 0.5$ perfect long-range order occurs where atom A has only B atoms as nearest neighbors and atom B has only A atoms as nearest neighbors.

C. Class III: Compositionally modulated alloys

Compositionally modulated alloys (CMA's) have a composition profile which varies periodically in a given direction with a wavelength that is commensurate with the lattice. The physical properties of CMA's have been found¹⁸ to deviate substantially from those of homogeneous alloys of similar average composition. Within a TB description, the Hamiltonian of compositionally modulated alloys can be written in the form of Eq. (2.1). A CMA can be characterized by the concentration of each species within a period of the modulation. For example, if the length of a period is three lattice spacings, we can use c_{A_1} , c_{A_2} , and c_{A_3} to parametrize the modulation, where the subscripts 1, 2, and 3 refer to consecutive planes within one period. The specific parameters we used in the various simulations of the ac conductivity of CMA's will be given explicitly in Sec. IV.

III. METHODOLOGY

In the numerical simulation of the DOS, we followed the common procedure of setting up a linear chain with the specified disorder characterized by specific values of the concentrations and the SRO parameters. The DOS was then calculated using the negative eigenvalue theorem¹⁹ for the infinite chain. This method is very efficient even for a linear chain with a large number ($\sim 10^6$) of atoms. In contrast, the frequency-dependent conductivity involves a dynamical process that requires the knowledge of both eigenvalues and eigenfunctions. The exact computation (without introducing a small imaginary number in the energy) of the ac conductivity by treating directly a linear chain with even a moderate number of atoms ($\sim 10^4$) is not feasible with today's computers. Approximations are needed to carry out the calculation.

In our simulations of the ac conductivity, we consider a linear chain as a collection of M segments of N atoms each, with M between 20 and 50, and N between 400 and 800. Each segment is taken to represent approximately a single configuration of the alloy. The number of configurations we used in our simulations depends on the size of a chosen frequency interval and the type of disorder considered.

The matrix elements of the Hamiltonian, Eq. (2.1), of a given configuration (with only nearest-neighbor interactions) are described by the relation

$$\langle i | H | j \rangle = \varepsilon_i \delta_{ij} = W_{ij} (\delta_{i,j+1} + \delta_{i+1,j}). \quad (3.1)$$

The Hamiltonian matrix can be directly diagonalized by

calculating the eigenvalues and eigenfunctions in the site representation. In this representation the eigenstate $|\mu\rangle$ can be expressed as a linear combination of the basis set of $\{|i\rangle\}$, where i refers to site i , namely

$$|\mu\rangle = \sum_i \langle i|\mu\rangle |i\rangle, \quad (3.2)$$

and $\langle i|\mu\rangle$ is the i th component of the eigenvector $|\mu\rangle$ in the site representation.

We applied, with appropriate modifications, the algorithm described in Ref. 13 to calculate the ac conductivity of a given configuration. Assuming the validity of linear-response theory, we evaluated the Kubo-Greenwood formula,

$$\text{Re}\sigma(\omega) = (2\pi e^2 a / L) \omega \sum_{\alpha, \beta} (f_\alpha - f_\beta) |\langle \alpha | x | \beta \rangle|^2 \times \delta(\hbar\omega + E_\alpha - E_\beta), \quad (3.3)$$

$$\text{Re}\sigma(\omega) = \frac{2\pi e^2 a}{\hbar} \frac{\hbar\omega}{N-1} \sum_{\alpha, \beta} [\Theta(\mu - E_\alpha) - \Theta(\mu - E_\beta)] \delta(\hbar\omega + E_\alpha - E_\beta) \left| \sum_{i=1}^N \langle i | \alpha \rangle i \langle \beta | i \rangle \right|^2, \quad (3.5)$$

where μ is Fermi energy and the Fermi distribution functions, at zero temperature, are replaced by the unit step function [$\Theta(x)=1$ for $x>0$ and $\Theta=0$ otherwise]. The ac conductivity can be computed directly from a knowledge of the eigenvalues and eigenvectors of a given segment.

For the case of short-range interactions, the Hamiltonians corresponding to segments larger than some minimum length should provide an adequate representation of a configuration of the entire chain. Finite-site effects also become negligible as the disorder increases and the eigenstates become more localized. We tested these conjectures by carrying out calculations for different combinations of M and N and judging against the rate of convergence of the averaged ac conductivity. The results were found to be stable for values of M and N of around 20 and 500, respectively. Thus the averaged conductivity converged to the ac conductivity of the original linear chain. A smoothing operation was finally performed because of the discreteness of the eigenvalues. The value of $\text{Re}\sigma(\omega)$ can only be defined at regularly spaced intervals of width $\Delta\omega$. The conductivity of a given interval was calculated as the integral

$$\text{Re}\sigma(\omega) = \frac{1}{\Delta\omega} \int_{\omega}^{\omega+\Delta\omega} \text{Re}\sigma(\omega') d\omega'. \quad (3.6)$$

This expression shows that the number of configurations needed to obtain a well-defined ac conductivity value depends on the size of $\Delta\omega$. Choosing a very small frequency interval either requires an impractically large number of configurations, or might cause the process to not converge to the right value. For each comparison we fixed the size of the frequency interval, choosing the intervals so that each contained at least four eigenvalues on the average. The number of configurations we used also varied with the type of disorder. We used 20 configurations for the

where x is the position operator for an electron in a chain of length L . E_α and $|\alpha\rangle$ are eigenvalues and eigenstates of H , i.e., $H|\alpha\rangle = E_\alpha|\alpha\rangle$, and f_α is the Fermi distribution function. The principal numerical task is the evaluation of the eigenvalues and eigenfunctions of the system under study. The dynamics is determined by the dipole transitions between two eigenstates associated with different energies.

In the tight-binding model we define the position operator x as

$$x = a \sum_i i |i\rangle \langle i|, \quad (3.4)$$

where a is the lattice spacing. The real part of the zero-temperature ac conductivity, Eq. (3.3), can then be reduced to the form

random case but 50 for the other cases. The final computer output is the average of the results over all configurations.

In summary, our simulation procedure is as follows.

- (1) Set up a linear chain with 20×500 (up to 50×500) atoms with the given parameters for the model Hamiltonian, Eq. (2.1).
- (2) Segment the chain into small configurations, each with 500 atoms.
- (3) Diagonalize the Hamiltonian matrix of each configuration by calculating the corresponding eigenvalues and eigenvectors.
- (4) Calculate the ac conductivity by using Eq. (3.5) with the smoothing procedure, Eq. (3.6).
- (5) Finally, average the ac conductivity over all configurations (segments).

IV. NUMERICAL RESULTS

Real materials are usually characterized by more than one of the various features of substitutional disorder defined in Sec. II. A satisfactory analytic theory should be general enough to calculate the transport quantities of all such materials. In this section we present and discuss the general features of our computer simulations for the ac conductivity of one-dimensional-model systems. Comparisons between analytic theories and the simulation results will be made in paper II.¹

The ac conductivity of linear chains with several types of disorder were calculated by using the procedure described in the preceding section. It was found that the number of configurations needed to obtain stable results depends on the type of disorder. For random, diagonally disordered systems we performed the average over 20 configurations, each configuration consisting of 500 atoms.

For other cases, in which the convergence was slower, 50 configurations were used. For each configuration the numerical work is straightforward involving the computation of eigenvalues and eigenvectors and the dipole transition matrix elements for different possible transitions.

All our simulations used two different scattering strengths for each type of disorder. For a binary alloy $A_{0.5}B_{0.5}$ with nearest-neighbor hopping, $W=1$, we considered two cases: In case I, weak scattering, we set $E_A = -E_B = 1.0$, i.e., $\delta=1$; and in case II, strong scattering, we set $E_A = -E_B = 2.0$, i.e., $\delta=2$. As we will see, localization effects are more prominent in case II, in which the simulation results show more spiky structure.

There are two main factors in the linear-response regime which dominate the contributions to the zero-temperature ac conductivity. One is the number of allowed dipole transitions among different levels, which is closely related to the joint DOS, and the other is the strength of the dipole transition matrix element $|\langle \alpha | x | \beta \rangle|^2$. The first contribution can be described by the available joint DOS

$$D(\omega) = \int_{\mu - \hbar\omega}^{\mu} dE \frac{1}{N^2} \sum_{\alpha, \beta} \delta(E - E_{\alpha}) \delta(E + \hbar\omega - E_{\beta}). \quad (4.1)$$

Notice that our definition of the available joint DOS is the contribution arising from the integration over the allowed range for photon-assisted transitions. Comparing Eq. (4.1) with Eq. (3.5), we conclude that the joint DOS does not describe completely the ac conductivity of alloys. The dipole transition matrix elements $|\langle \alpha | x | \beta \rangle|^2$ will have dominant contributions to the ac conductivity when the energy difference $|E_{\alpha} - E_{\beta}|$ is large. In Fig. 1 we show the DOS spectrum, the joint DOS, and the ac conductivity spectrum for a strong scattering case. The structure of the joint DOS, Fig. 1(b), and the ac conductivity spectrum (the real part) can be understood in broad terms by the spectrum of the DOS, Fig. 1(a). The main structure of the ac conductivity spectrum consists of two main peaks separated by a dip at $\omega=0.5$. The dip is due to the gaps in the DOS, $n(E)$, at $E = \pm 2.0$, while the peaks in $\sigma(\omega)$ correspond to the structure in $n(E)$ above and below those gaps. The ac conductivity, Fig. 1(c), decreases much faster than the available joint DOS at higher frequencies which reflects the effects of the dipole transition matrix elements.

In all our conductivity spectra, the average conductivities are given in units of $2\pi e^2 a / \hbar$, and the frequency is given in units of the whole bandwidth. The frequency interval $\Delta\omega$ used in the smoothing procedure is equal to $\frac{1}{120}$ of the corresponding bandwidth. Each interval range contains four eigenvalues on the average for a configuration of 500 atoms. We now discuss the qualitative features of our simulation results according to the order in which the models were defined in Sec. II.

A. Class I: Random disorder

1. Binary alloys

(a) *Diagonal disorder.* The DOS spectra are symmetric with respect to the middle of the band for both the weak

and strong scattering cases defined above; for the case of strong scattering, this is shown in Fig. 1(a). This symmetry is reflected in the ac conductivity spectra as functions of the Fermi energy, μ , which are symmetric about $\mu=0.5$. For example, the spectrum for the case $\mu=0.2$ is identical to the spectrum for the case $\mu=0.8$ and provides a direct check on the reliability of the smoothing operation used in the numerical calculations. The top row of Fig. 2 depicts the spectra of the weak scattering case for $\mu=0.2, 0.4$, and 0.5 . The bottom row of Fig. 2 shows the analogous results for case II (strong scattering). Two important features appear in these figures: The spectra for

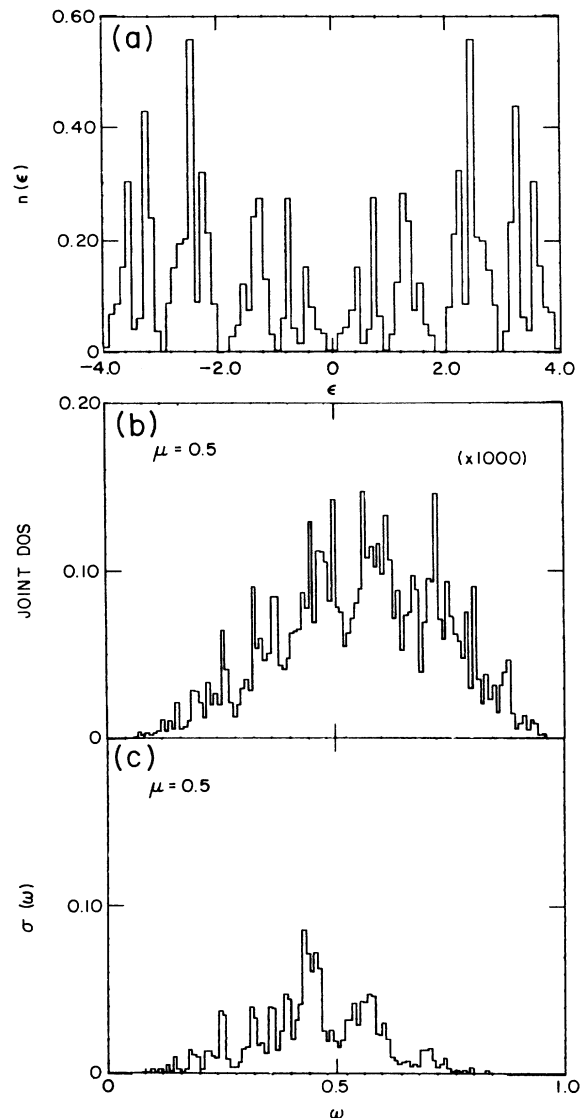


FIG. 1. Exact computer-simulation results for the case of a strong scattering binary alloy $A_{0.5}B_{0.5}$ with $E_A = -E_B = 2.0$, $W=1.0$: (a) density of states, (b) joint density of states per number of atoms squared, and (c) average ac conductivity. The Fermi energy is at the middle of the band, i.e., $\mu=0.5$, and the frequency is in units of bandwidth.

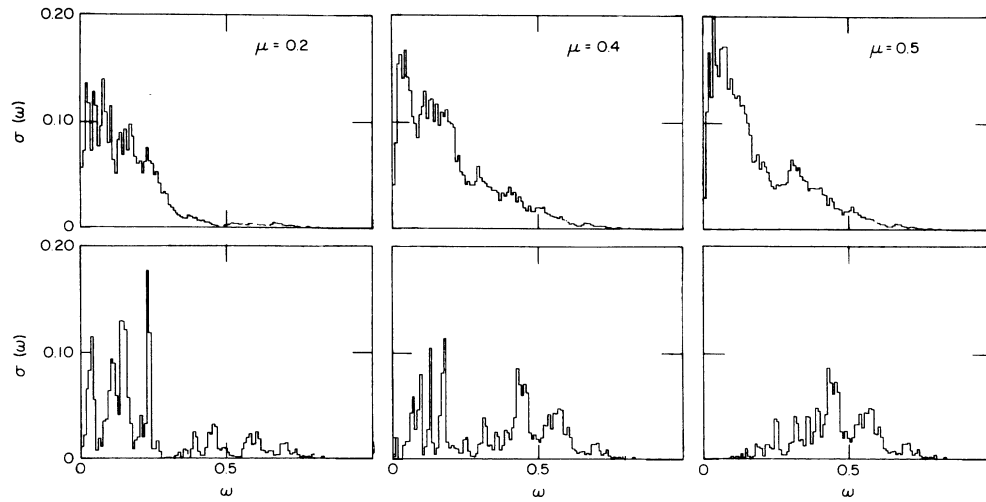


FIG. 2. Average ac conductivity of random binary alloys, $A_{0.5}B_{0.5}$ for three values of the Fermi energy μ labeling the columns from left to right. Top row, weak scattering alloys, $\delta=1.0$ (case I); bottom row, strong scattering alloys, $\delta=2.0$ (case II). The scattering strength δ is defined in Eq. (2.2), and cases I and II are defined in Sec. IV.

the weak scattering cases resemble the spectrum of a pure system, i.e., peak centered at zero frequency. When the disorder increases, the peak at the origin shifts to higher frequency and the magnitude of the ac conductivity decreases. As is well known,²⁰ even the slightest amount of disorder suffices to localize completely the states in a one-dimensional system. It follows that the dc conductivity should vanish for one-dimensional substitutionally disordered alloys. As already mentioned, it requires a large sample size¹¹ to obtain reliable results for the dc conductivity of disordered systems. Therefore, we did not attempt to calculate the ac conductivity near $\omega \approx 0$. The smallest frequency ω we used is $\frac{1}{80}$ of the whole bandwidth.

(b) *Off-diagonal disorder.* In order to see both the effects of pure off-diagonal disorder, and the effects of mixing diagonal and off-diagonal disorder, we carried out two different computer simulations for off-diagonally disordered alloys. Here, the fluctuations in the hopping pro-

cess cause slower convergence than in the purely diagonal disorder case. The results of Fig. 3 were obtained by averaging the ac conductivity over 50 configurations. The off-diagonal effects also make the DOS spectra, and in turn the conductivity spectra, asymmetric. Thus the results are presented over a broader frequency range for the Fermi energy than for diagonally disordered systems, i.e., $\mu=0.2, 0.4, 0.5, 0.6$. The results in the top row of Fig. 3 correspond to systems with both diagonal and off-diagonal disorder, whereas those in the bottom row correspond to systems with only ODD. Comparison of the two rows shows clearly that strong diagonal disorder increases dramatically the structure in the ac conductivity curves, as it is known to do in the DOS curves.

2. Ternary alloys

It is interesting to observe the effects in the conductivity spectrum when the number of alloy components is in-

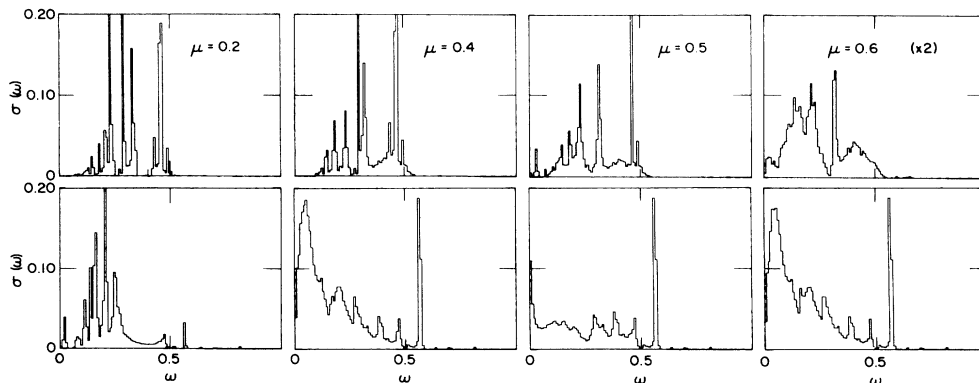


FIG. 3. Average ac conductivity of binary $A_{0.5}B_{0.5}$ alloys with ODD. Top row, alloys with both diagonal and off-diagonal disorder, $E_A = -E_B = 2.0$, $W_{AA} = 0.5$, $W_{AB} = 1.0$, and $W_{BB} = 2.5$. Bottom row, alloys with only off-diagonal disorder $E_A = E_B = 0.0$, $W_{AA} = 0.5$, $W_{AB} = 1.0$, and $W_{BB} = 2.5$.

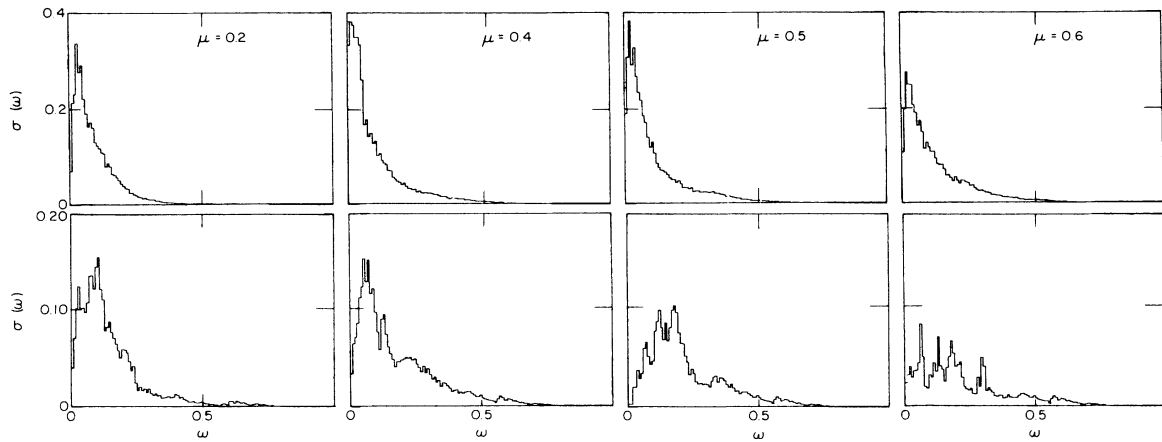


FIG. 4. Average ac conductivity of ternary alloys, $A_{0.1}B_{0.3}C_{0.6}$ with only diagonal disorder. Top row, weak-scattering alloys, $E_A = -E_B = 1.0$, $E_C = 0.0$, and $W = 1.0$. Bottom row, strong scattering alloys, $E_A = -E_B = 2.0$, $E_C = 0.0$, and $W = 1.0$.

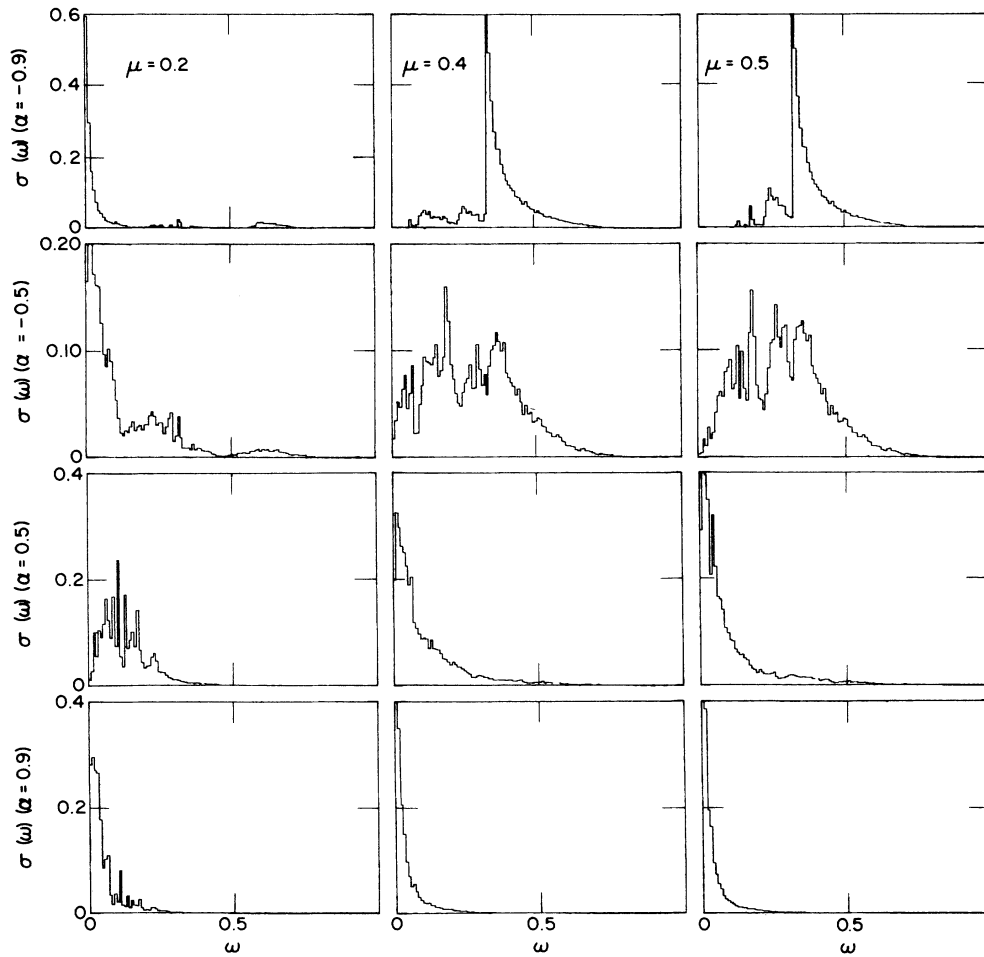


FIG. 5. Average ac conductivity of alloys with only diagonal disorder and nonvanishing short-range order. The rows in the figure are labeled by the parameter α defined in Sec. II; the alloy parameters are those of case I (weak scattering) described in Sec. IV.

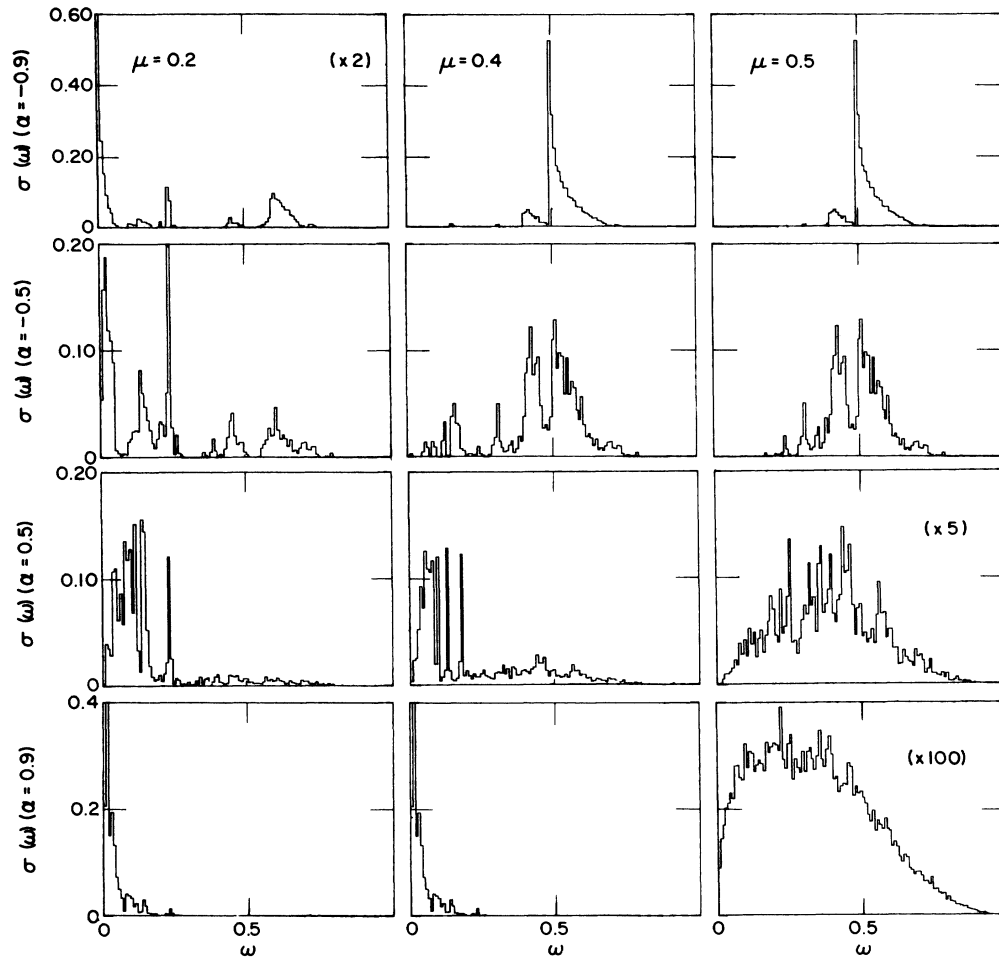


FIG. 6. Results analogous to those shown in Fig. 5 but for case II (strong scattering).

creased from two to three. The figures in the top row of Fig. 4 are the results obtained for the weak scattering case of a ternary alloy. Here, we set $E_A = -E_B = 1.0$, $E_C = 0.0$, $W = 1.0$, and $c_A = 0.1$, $c_B = 0.3$, $c_C = 0.6$. For the figures in the bottom row of Fig. 4 the values of E_A and $-E_B$ were changed to 2.0 while other parameters were kept the same.

Once again, increased disorder results in increased structure in the ac conductivity spectra for ternary alloys as it does in the case of binary alloys. However, there seems to be comparatively less structure in the ac conductivity associated with ternary than binary systems. This is not a general result. It is simply due to the fact that for the parameters chosen in the former case the alloy DOS is somewhat smoother than for the two-component alloys, resulting in an increased number of allowed dipole transitions. Clearly, an increase in scattering strength would lead to increased structure in the ac conductivity spectra. Finally, also in this case the dc conductivity $\sigma(0)$ appears to vanish within the accuracy of the calculations.

B. Class II: Short-range order

In order to check the validity of the extension of analytic theories to alloys with short-range order, we carried out ac conductivity simulations for different degrees of non-randomness. The ordering parameter α used is defined in Sec. II. We considered the effect due to SRO, from the almost complete clustering case ($\alpha = 0.9$) to the almost complete ordering case ($\alpha = -0.9$) in four steps: $\alpha = 0.9, 0.5, -0.5, -0.9$. At each step, calculations for three different values of the Fermi energy, $\mu = 0.2, 0.4, 0.5$, were carried out. Figure 5 shows the results for the weak scattering case, and Fig. 6 for the strong scattering case. The parameters used in these calculations are given in the figure captions.

We note that stronger scattering alloys, Fig. 6, produce more structured ac conductivity spectra than weak-scattering systems, Fig. 5, for almost all degrees of SRO, i.e., values of the parameter α . An important exception to this observation is afforded by the case of strongly order-

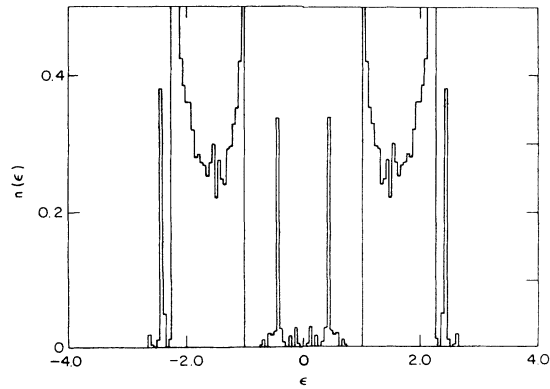


FIG. 7. Densities of states for case II (strong scattering) and strong ordering alloy, $\alpha = -0.9$.

ing alloys, $\alpha = -0.9$, shown in the top rows of Figs. 5 and 6. The two sets of figures appear to be correspondingly identical. This effect can be understood qualitatively in terms of the joint DOS for strongly ordered alloys, an example of which is shown in Fig. 7. For a value of $\mu = 0.5$, the joint DOS consists of practically a single peak resulting from the narrow structures in the DOS centered at $E = \pm 2.0$.

This is indeed the result reflected in the upper right-hand panels of Figs. 5 and 6. The remaining features of the various curves in these figures can be understood along similar lines.

C. Class III: Compositionally modulated alloys

The results for the ac conductivity of compositionally modulated alloys are presented in Figs. 8 and 9. The CMS's considered were characterized by a modulation

wavelength of three lattice spacings with corresponding concentrations c_{A_1} , c_{A_2} , c_{A_3} , and $c_{B_i} = 1 - c_{A_i}$ for $i = 1, 2, 3$. For weakly modulated alloys, Fig. 8, the values $c_{A_1} = 0.3$, $c_{A_2} = 0.5$, and $c_{A_3} = 0.7$ were chosen, while for strongly modulated alloys, Fig. 9, we set $c_{A_1} = 0.1$, $c_{A_2} = 0.5$, and $c_{A_3} = 0.9$. For each modulated strength, we considered alloys characterized by weak scattering, $\delta = 1$, as well as by strong scattering, $\delta = 2$. The results for the weak-scattering alloys are shown in the top rows of Figs. 8 and 9, while those for strongly scattering alloys are depicted on the bottom rows.

Several of the features exhibited by the curves in these figures are quite similar and analogous to those associated with the random alloys of comparable strength, Fig. 2. On the other hand, increased modulation strength appears to increase the structure in the ac conductivity curves, as is seen immediately by comparing Figs. 8 and 9 with Fig. 2. For example, note the prominent peak at $\omega \approx 0.5$ in the lower right-hand panel of Fig. 9, and compare this with the relatively weak structure in the corresponding panel of Fig. 2. These features can be understood simply in terms of the DOS's of CMA's (Ref. 8) in complete analogy with the case of random alloys.

Recently, Saso *et al.*¹⁴ applied the recursive method to investigate the low-frequency behavior of the dynamical conductivity, $\sigma(\omega)$, for electrons on very long (10^6 sites) disordered chains. They established that at low frequency the analytic results originally established by Berezinskii²¹ are asymptotically exact in the limit of weak disorder. Their results naturally explain the failure of the first computer experiment¹² mentioned in the Introduction. We also applied the recursive algorithm to calculate the ac conductivity of model systems and obtained reasonable agreement with the results obtained by the method of Ref. 17. One typical result is given in Fig. 10 for a strong scattering alloy ($\delta = 2.0$, case II) and $\mu = 0.5$. It is easily

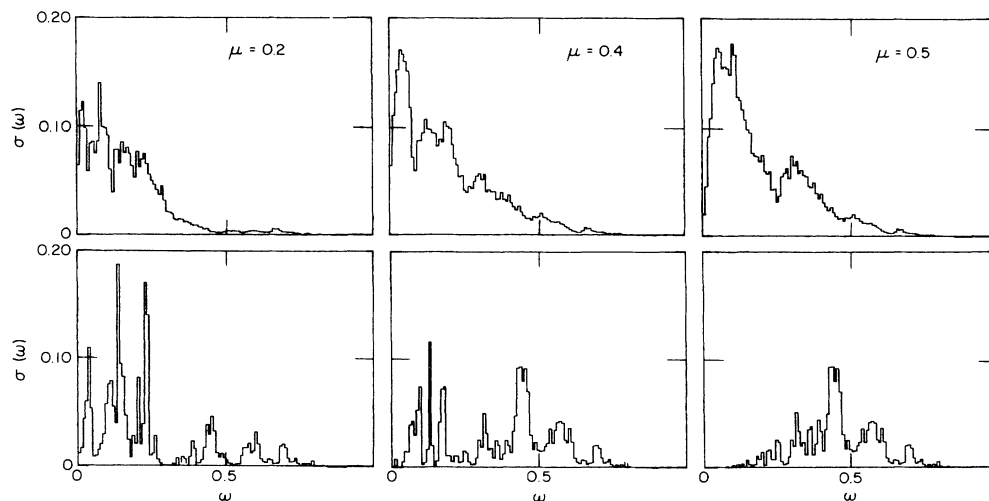


FIG. 8. Average ac conductivity of weakly modulated alloys, $C_{A_1} = 0.3$, $C_{A_2} = 0.5$, and $C_{A_3} = 0.7$, for case I (top row) and case II (bottom row).

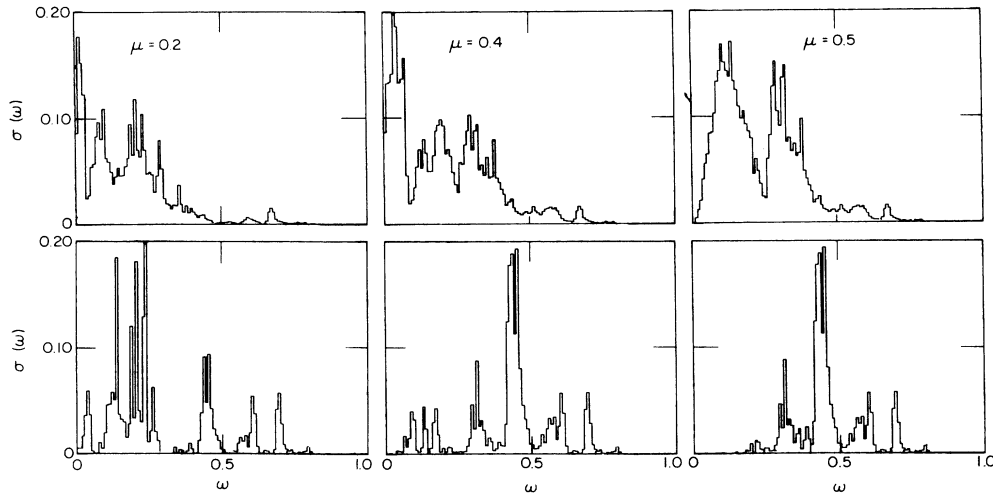


FIG. 9. Results of the type depicted in Fig. 8, but for strongly modulated alloys, $C_{A_1}=0.1$, $C_{A_2}=0.5$, and $C_{A_3}=0.9$.

seen that in this case the agreement between the results obtained by the two methods is excellent. However, the peaks in Fig. 10 obtained by the recursive technique (histogram) are very pronounced and their widths depend rather strongly on the small imaginary number γ used in the energy, i.e., $E \rightarrow E + i\gamma$, which in general makes quantitative comparison somewhat difficult.

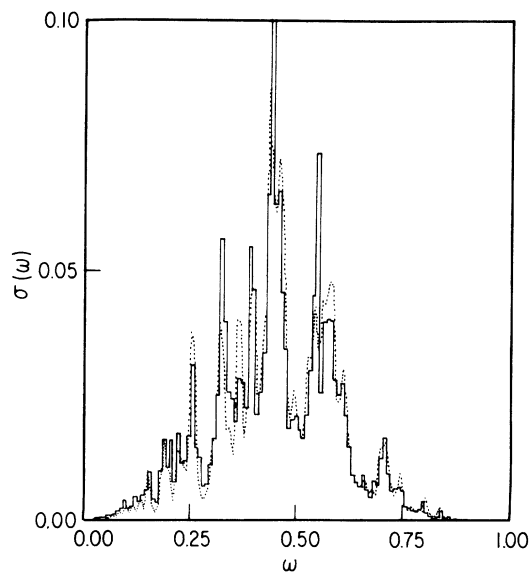


FIG. 10. Comparison of typical $\sigma(\omega)$ spectra obtained with the recursive method (histogram) and by the method of Ref. 13. The parameters used are $\delta=2.0$ (case II), $\mu=0.5$, and $\gamma=0.001$ in the recursive algorithm. The sample size is 10 000 sites.

V. DISCUSSION AND CONCLUSIONS

We have presented exact computer-simulation results for the ac conductivity of one-dimensional substitutionally disordered alloys characterized by various types of disorder. Our aim is to provide a comparative basis on which one can test the validity of analytic but approximate methods for calculating the transport properties in disordered materials. Some of the comparisons will be reported in II.

Our results are rigorously valid at zero temperature. The simulation of the ac conductivity for a system at finite temperature can be easily obtained by extending the formalism of this paper. In that case, however, the effect of electron-phonon scattering must be included in the Kubo-Greenwood formula. It will be interesting to observe the competing effect between the electronic and vibrational structure through computer simulations. Simulations for multiband or higher-dimensional-model systems are also feasible, which would yield results that can be used to probe the transport properties of these systems.

In the past, results of computer simulations for the DOS's have been helpful in assessing the weaknesses and strengths of approximate theories like the CPA (Refs. 2 and 3) and its generalizations (Refs. 4–8). We expect that the ac conductivity simulation results will play a similar role in calibrating the application of the CPA and its extensions to the calculation of the ac conductivity. Our analytic calculations for the ac conductivity of model systems show that the single-site CPA theory gives average results but cannot reproduce the fine structure which appears in many ac conductivity spectra. Such structure is caused primarily by correlation effects which cannot be taken into account within the single-site CPA theory. In

order to take correlation effects into account a multisite or cluster extension of the CPA is needed. Such cluster extensions would allow the calculation of the vertex corrections which are often quite important and should be included properly. The simulation results presented here have been useful for understanding the structure of vertex corrections and directing our analytic cluster calculations which are reported in II.

ACKNOWLEDGMENT

This work was supported by the National Science Foundation through the Northwestern University Materials Research Center (Division of Materials Research Grant No. DMR-82-16972) and by a grant of supercomputing time by the National Science Foundation (NSF) Office for Advanced Scientific Computing.

-
- ¹M. Hwang, A. Gonis, and A. J. Freeman, following paper, Phys. Rev. B **35**, 8985 (1987), referred to as II.
- ²P. Soven, Phys. Rev. **156**, 809 (1967); **178**, 1136 (1969); D. W. Taylor, *ibid.* **156**, 1017 (1967).
- ³B. Velický, S. Kirkpatrick, and H. Ehrenreich, Phys. Rev. **175**, 747 (1968).
- ⁴M. Tsukada, Phys. Soc. Jpn. **26**, 684 (1969); **32**, 1475 (1972).
- ⁵W. H. Butler, Phys. Rev. B **8**, 4499 (1973).
- ⁶A. Gonis and J. W. Garland, Phys. Rev. B **16**, 242 (1977).
- ⁷A. Gonis, G. M. Stocks, W. H. Butler, and H. Winter, Phys. Rev. B **29**, 555 (1984).
- ⁸A. Gonis and N. K. Flevaris, Phys. Rev. B **25**, 7544 (1982).
- ⁹We shall refer explicitly to several such approximate methods as it becomes appropriate in the following papers.
- ¹⁰Some examples: H. Neddermeyer, in *Electrons in Disordered Metals and at Metallic Surfaces*, edited by P. Phariseau *et al.* (Plenum, New York, 1978), p. 293–322; S. Tanaka, Normal and Superconducting Parameters of BaPb_{1-x}Bi_xO₃, Proceedings of the International Conference on Materials and Mechanisms of Superconductivity, Ames, 1985 (unpublished).
- ¹¹D. J. Thouless and S. Kirkpatrick, J. Phys. C **14**, 235 (1981).
- ¹²C. M. Penchina and P. C. Mitchell, J. Non-Cryst. Solids **7**, 127 (1972).
- ¹³R. C. Albers and J. E. Gubernatis, Phys. Rev. B **17**, 4484 (1978).
- ¹⁴T. Saso, C. I. Kim, and T. Kasuya, J. Phys. Soc. Jpn. **52**, 1888 (1983); T. Saso, J. Phys. C **17**, 2905 (1984).
- ¹⁵B. Velický, Phys. Rev. **184**, 614 (1969).
- ¹⁶G. Czycholl and J. Zittartz, Z. Phys. B **30**, 375 (1978).
- ¹⁷F. Brouers and A. V. Vedyayev, Phys. Rev. B **2**, 348 (1972).
- ¹⁸I. Schuller, C. M. Falco, J. E. Hilliard, J. Ketterson, B. Thaler, R. Lacoé, and R. Dee, in *Modulated Structures—1979 (Kailua Kona, Hawaii)*, Proceedings of the International Conference on Modulated Structure, edited by J. M. Cowley, J. B. Cohen, M. B. Salamon, and B. J. Wuensh (AIP, New York, 1979), p. 417; W. M. C. Yang, T. Tsakalakos, and J. E. Hilliard, J. Appl. Phys. **48**, 876 (1977).
- ¹⁹P. Dean, Rev. Mod. Phys. **44**, 127 (1972).
- ²⁰R. Lanauer, Philos. Mag. **21**, 863 (1970); P. W. Anderson, E. Abrahams, and T. V. Ramakrishnan, Phys. Rev. Lett. **43**, 718 (1979).
- ²¹V. L. Berenzinskii, Zh. Eksp. Teor. Fiz. **65**, 1251 (1973) [Sov. Phys.—JETP **38**, 620 (1974)].